Environ Sci Pollut Res (2015) 22:2076–2086
DOI 10.1007/s11356-014-3499-y

RESEARCH ARTICLE

Rare earths exposure and male infertility: the injury mechanism study of rare earths on male mice and human sperm

Jun Chen · Heng-jun Xiao · Tao Qi · Di-ling Chen · He-ming Long · Song-hao Liu

Received: 14 April 2014 / Accepted: 20 August 2014 / Published online: 30 August 2014
© Springer-Verlag Berlin Heidelberg 2014

Abstract The weight; testis/body coefficient; levels of LDH, SDH, SODH, G-6PD, and testosterone; cell cycle; and cell apoptosis of the male mice were influenced after being treated with 200 mg/[kg/day] of rare earths suspension for 3 weeks. The "Raman fingerprints" of the human sperm DNA exposed to 0.040 mg/ml $CeCl_3$ were very different from those of the untreated; the Raman bands at 789 cm^{-1} (backbone phosphodiester), PO_4 backbone at 1,094 cm^{-1}, methylene deformation mode at 1,221 cm^{-1}, methylene deformation mode at 1,485 cm^{-1}, and amide II at 1,612 cm^{-1}, of which intensities and shifts were changed, might be the diagnostic biomarkers or potential therapeutic targets. The injury mechanism might be that the rare earths influence the oxidative stress and blood testosterone barrier, tangle the big biomolecule concurrently, which might cause the testicular cells and vascular system disorder and/or dysfunction, and at the same time change the physical and chemical properties of the sperm directly.

Keywords Rare earth elements · Reproduction toxicity · Sperm · Male infertility · Confocal micro-Raman spectroscopy

Responsible editor: Philippe Garrigues

Jun Chen and Heng-jun Xiao equally contributed to the article.

J. Chen · T. Qi
Department of Infertility and Sexual Medicine, The Third Affiliated Hospital of Sun Yat-sen University, Guangzhou, Guangdong 510631, China

J. Chen · S.-h. Liu
School of Information and Optoelectronic Science and Engineering, South China Normal University, Guangzhou, Guangdong 510006, China

H.-j. Xiao
Department of Urology, The Third Affiliated Hospital of Sun Yat-sen University, Guangzhou, Guangdong 510631, China

D.-l. Chen (✉)
Guangdong Institute of Microbiology, Guangzhou, Guangdong 510070, China
e-mail: diling1983@163.com

H.-m. Long
Department of Oncology, The First Affiliated Hospital of Gannan Medical University, Ganzhou, Jiangxi 341000, China

Introduction

The rare earths reserve in China is the highest all over the word and is widespread throughout 18 provinces and cities. The average level of rare earths in the Chinese soil is quite the same with that all over the world; much of the constituents were light rare earths, especially cerium content, which accounts for 42 % of the total and 48 % of the light rare earths (Liu et al. 2007, 2013a, b; Zhang et al. 2009; He et al. 2004; Xu et al. 2012). There are two characteristics of the concentration of rare earths in the Chinese river. First, the content is higher in which the average concentration of lanthanum, cerium, neodymium, terbium, and ytterbium in Chinese freshwater river is more than two times higher than that of the world. The second is uneven distribution; for example, the content in the southern part of Jiangxi (one of the two higher-resource provinces in China) is significantly higher than that in the lake water system. Simultaneously, survey data analyzed from more than 30 different main foods as grain, vegetable, melon, and fruit covered 17 provinces or cities, and based on the normal daily food intake of the resident in China, showed that the average dietary intake of rare earths for each person in China is 2.10~2.50 mg/day; but in southern Jiangxi, the dietary intake from the area of heavy rare earths, light rare earths, and control were 6.67, 5.98, and 3.33 mg/day, respectively, which exceeds much more than the allowed intake (Wei et al. 2009; Wu et al. 2011; Wei et al. 2001; Su et al. 1993; Li et al. 2012; Pang et al. 2002; Zhang and Shan 2001; Jiang et al.

2012; Zhang et al. 2001). All showed that rare earths pollution is becoming a serious potential factor for food-borne diseases for the mining-area residents in China.

Because of its unique structure and performance, widespread use of rare earths is increasing in the industrial and agricultural production over the past 20 years. Although, in general or for a certain period, rare earths exposure does not show obvious harm to the body, long-term and excessive exposure or ingestion may cause adverse consequences to human health or metabolism (Peng et al. 2003; Tong et al. 2004; Fan et al. 2004; Yu et al. 2004, 2007; Zhou et al. 2012, 2013; He and Xue 2005; Liu et al. 2012; Boenigk et al. 2005; Gardner et al. 1997). Toxicology research on animal experiments found that rare earths are an obvious toxic agent for the liver and interfere with the metabolism of sugar, fat, protein, nucleic acid, or even drugs. It is a coupling factor of excited-contraction in the muscular system, an uncoupling factor of stimulation-excretion in the neuroendocrine system, an inhibitor on many clotting factor that can prolong coagulation time, and a control agent on the release and uptake of the neurotransmitter. Researches also show that they have some effect on the reproductive system (Levack et al. 2002; Friel et al. 1999), but more evidence is still needed.

Although the male fertility is a complex process, environmental causes were included. Overexposure to certain environmental elements such as heat, toxins, chemicals, heavy metal exposure, radiation, or X-rays and frequent use of saunas or hot tubs may temporarily lower the sperm count and reduce sperm production or sperm function. For unordered exploitation and utilization, much of the rare earths were considered as widespread environmental and occupational contaminants with mutagenic, carcinogenic, and teratogenic effects, so the adverse consequences of rare earths to the human health needs more urgent studies. To investigate whether rare earths do harm the male fertility, we prepared the intragastric administration of rare earths-polluted male mice model; tested the changes of weight, testis/body coefficient, levels of lactate dehydrogenase (LDH), succinate dehydrogenase (SDH), sorbitol dehydrogenase (SODH), glucose-6-phosphate dehydrogenase (G-6PD), testosterone, cell cycle and cell apoptosis, and the human sperm exposure to cerium trichloride in vitro; then, observed the changes of the antioxidant power and the sperm structure to reveal the injury mechanism of rare earths on male infertility and to help correct early clinical diagnosis and find some targets or new drugs for the treatment.

Materials and methods

Mice and drug treatment procedures

Adult male Kunming mice (18–22 g, obtained from the Center of Laboratory Animal of Guangzhou University of Chinese Medicine, SCXK [Yue] 2008-0020, SYXK [Yue] 2008-0085) were housed in pairs in plastic cages in a temperature-controlled (25 °C) colony room on a 12/12-h light/dark cycle. The mice were fed a standard diet and water was available ad libitum. All experiment protocols were approved by the Center of Laboratory Animals of Guangzhou University of Chinese Medicine. All efforts were made to minimize the number of animals used.

The mice were randomly divided into four groups as follows: normal control group (received oral distilled water), low-dose group (irrigate 100 mg/[kg·day], medium-dose group (200 mg/[kg·day]), and high-dose group (400 mg/[kg·day]) of rare earth suspension. The rare earth was purchased from Ganzhou Haoxiang New Materials Co., Ltd. (China), dissolved in phosphate-buffered saline solution with a concentration of 400 mg/mL, and stored at 4 °C before being used. Normal saline and medicinal alcohol were purchased from WJ Biotechnology (China)). Every group had eight animals, and the experiments lasted 21 days.

Human sperm preparation

The experiment was approved by the ethics committee of the Third Affiliated Hospital of Sun Yat-sen University, and written informed consent was obtained from 13 healthy donors who provided semen samples after 2–5 days of sexual abstinence. Light microscopic analysis, according to WHO recommendations (World Health Organization, 1999), showed all parameters to be above normal limits. Samples were divided into two, half were kept in seminal plasma ("native"), and the remainder were diluted in excess phosphate-buffered saline (PBS), centrifuged at 400 g for 10 min; the supernatant was removed; and the pellet was resuspended in fresh PBS ("washed"). Half of the washed sample was then exposed to cerium trichloride at 37 °C for 45 min, the other half was left untreated. All aliquots were frozen in liquid nitrogen and stored prior to use. Half of the sperm samples exposed to cerium trichloride were centrifuged at 400 g for 10 min, and then were placed on an aluminum slice for Raman scanning.

Enzymatic assays

Skin over the neck region was excised open immediately after anesthesia, and blood was drawn from the common carotid artery using a 5-mL syringe and needle. Blood sample was centrifuged at 3,000 rpm for 10 min using a bench centrifuge, and the collected serum was stored at 4 °C before assay was carried out. The enzyme-linked immunoabsorbent assay (ELISA) technique (TECO Diagnostics, Anaheim, CA, USA; Biotech Laboratory Ltd, UK) was used to assay for testosterone.

The activities of malondialdehyde (MDA), superoxide dismutase (SOD), glutathione reductase (GSH-Px), LDH, SDH,

G-6PD, and SODH were measured with detection kits (Aly and Azhar 2013; Traina et al. 2003; Pant et al. 1995). Protein concentration was determined using the Coomassie Brilliant Blue G250 assay. The kits were all purchased from Nanjing Jiancheng Bioengineering Institute (Nanjing, Jiangsu, China). The procedures were performed according to the manufacturer's instructions. Levels were normalized to the protein concentration of each sample and expressed as a percentage of nontreated controls. All other reagents and chemicals used in the study were of analytical grade.

Cell cycle and cell apoptosis of sperm determination

Cell cycle and cell apoptosis of sperm determination were measured by flow cytometry (FCM) using propidium iodide (PI) staining. The experimental procedure was as follows: the testis were dissected and added to 2 mL precooled saline, homogenized in an ice bath, filtered with cell strainers, and centrifuged for 10 min at 1,200 r/min. The supernatant was removed, 1.5 mL PBS solution was added and dispersed, the sample was filtered again, centrifuged for 5 min at 1,200 rpm, and the supernatant was discarded. Finally, we added 2 mL 70 % ethanol for storage at 4 °C for 24 h. Then, the sample was centrifuged, the supernatant was discarded, 1 mL PBS was added, the sample was centrifuged for 5 min at 1,500 r/min, the supernatant was removed, 200 μL PBS and 200 μL PI dye was added, incubated in the dark for 20 min at 4 °C, and then measured in a flow cytometer (CytomicsTM FC 500, Beckman Coulter, USA) at Ex 488 nm and Em 630 nm.

Raman spectra

Raman spectra were acquired using a Via Plus laser Micro-Raman spectroscopy system purchased from the Renishaw Company. The resolution of this instrument is 1 cm^{-1}.

For the testis scanning, after being treated for 21 days, the rats were put to death by abdominal aorta bloodletting after anesthesia. The testis were dissected, washed with normal saline, and then fixed in field with 4 % paraformaldehyde solution. The testis tissues were transversely sectioned and placed on a silicon slice for Raman scanning. There were no extra Raman peaks in the 900 to 2,000 cm^{-1} region of the silicon slice. All the Raman spectra were recorded for 10 s and five accumulations. The 785-nm laser was chosen, and 5 % of the exposed laser was much lower than the safe exposure limit.

For human sperm scanning, all the Raman spectra were recorded for 30 s and three accumulations. The 514-nm laser was chosen, and 100 % of the 15-W exposed laser of was much lower than the safe limit of exposure; there were no obvious Raman peaks in the 350 to 2,200 cm^{-1} region on the aluminum slice.

All the data were collected under the same conditions, the background was corrected, and the instrument was calibrated by silicon at the 520 cm^{-1} band.

Data analysis

In order to compare the related spectrum changes. At least five spectra were obtained from each sperm around the head and 10 for each sample. Then, the spectrum was baseline corrected by the R2.8.1 software (provided by Renishaw), smoothed, normalized, and averaged by Origin 8.0 (OriginLab Crop., Northampton, MA, USA). Statistical Package for the Social Science (SPSS 17.0, SPSS Inc) was used for the statistical analysis in this study.

The recorded spectra were statistically analyzed by principal component analysis (PCA). Other obtained data were analyzed using Student's t test to compare variables and ANOVA with Turkeys post hoc test to compare between the groups. The results expressed as mean±SD ($p<0.05$) were considered significant.

Results and discussion

Organ/body coefficient of testis

As shown in Fig. 1a, the weight of the high- and medium-dose groups slowly grew after being exposed for 21 days ($p<0.05$, compared to the normal group), while the low dose is strictly the same with the normal group, which indicated that short-term rare earths exposure does not obviously harm body growth, but long-term exposure or ingestion may have adverse consequences to body growth or metabolism. In Fig. 1b, the testis of the organ/body coefficient of the exposed groups (400, 200, and 100 mg/[kg·d]) were decreased to 88.25, 91.28, and 97.86 %, respectively. The difference of the high-dose group was significant ($p<0.01$, compared to the normal group), which indicated that pathological changes have occurred on the testis of the rare earths-exposed male mice.

Enzymatic assays

LDH, which mainly exist in the spermatocyte, cytoplasm, and mitochondria of the sperm cell, is the catalyst that converts pyruvate into lactic acid for anaerobic metabolism and is the important enzyme of the glycolysis to provide energy after meiosis pachytene of the spermatocyte and is associated with the maturity of spermatogenic epithelium. The levels of LDH in testis (exposed to 400, 200, and 100 mg/[kg·day]) were decreased to 81.18, 88.87, and 97.31 %, respectively. The difference of the high-dose group was significant ($p<0.01$, compared to the normal group) as shown in Fig. 2a. The levels

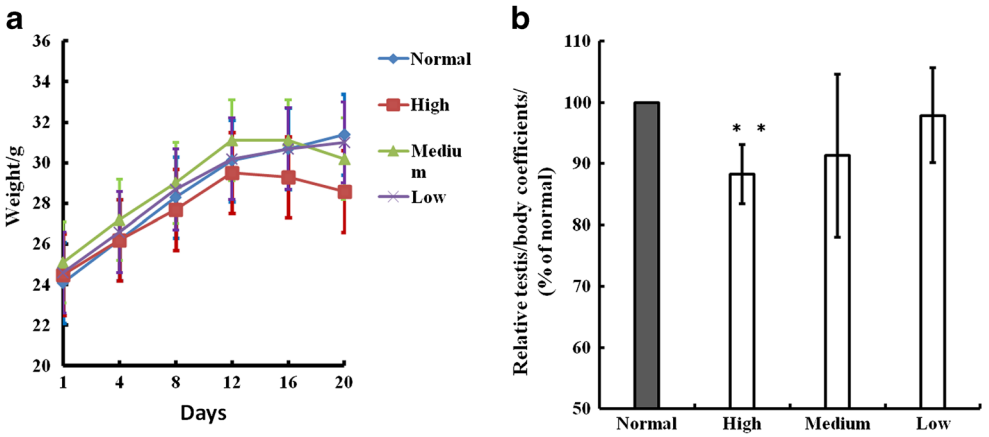

Fig. 1 Effect of weight and testis/body coefficients in the rare earths-exposed male mice. The graphic of **a** is the effect of weight, **b** is the effect of testis/body coefficients, and normal group received oral distilled water, low-dose group irrigate 100 mg/[kg·day] of rare earth suspension, medium-dose group irrigate 200 mg/[kg·day], and high-dose group irrigate 400 mg/[kg·day]. Values given are the mean±SD (n=8); $^{*}p$<0.05 vs normal group, $^{**}p$<0.01 vs normal group

of SDH, SODH, and G-6PD showed the same trend except the increase of the SODH and G-6PD levels at the low-dose group as shown in Fig. 2.

As shown in Fig. 3a, the levels of serum testosterone (exposed to 400, 200, and 100 mg/[kg·day]) were decreased to 17.08, 70.77, and 94.59 %, respectively. The difference of medium- and high-dose group was significant (p<0.01, compared to the normal group).

As shown in Fig. 3, after culture with $CeCl_3$ (0.004, 0.040, and 0.400 μg/ml), the levels of SOD (Fig. 3b) and GSH-Px (Fig. 3c) markedly drop, and the levels of MDA (Fig. 3d) sharply increased, which showed significant differences (p<0.05) compared with the normal control group. The results suggested that Ce^{3+} cause oxidative damage and destroy the antioxidant defense systems of the sperm, and even lead to damage or

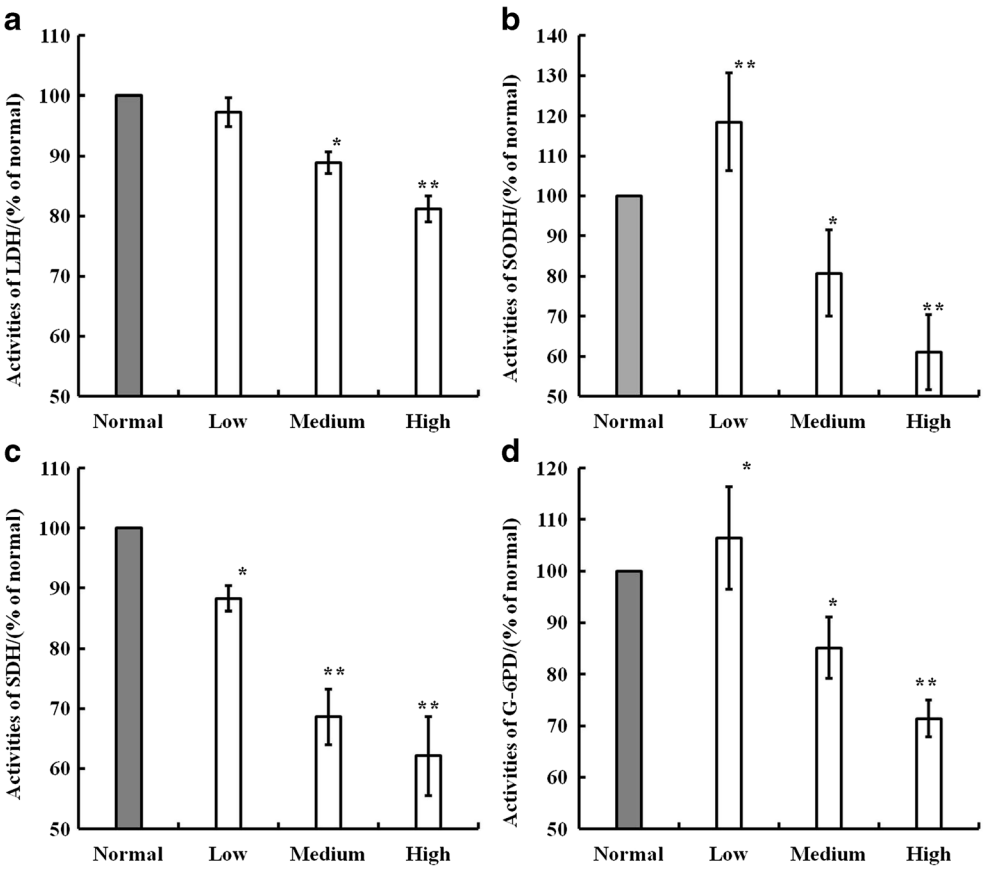

Fig. 2 Effect of rare earths on enzymatic activities of testis in male mice. The graphic of **a** is the activities of LDH, **b** SODH, **c** SDH, and **d** G-6PD, normal group (received oral distilled water), low-dose group (irrigate 100 mg/[kg·day] of rare earth suspension), medium-dose group irrigate 200 mg/[kg·day], and high-dose group irrigate 400 mg/[kg·day]. Values given are the mean±SD (n=8), $^{*}p$<0.05 *vs* normal group, $^{**}p$<0.01 *vs* normal group

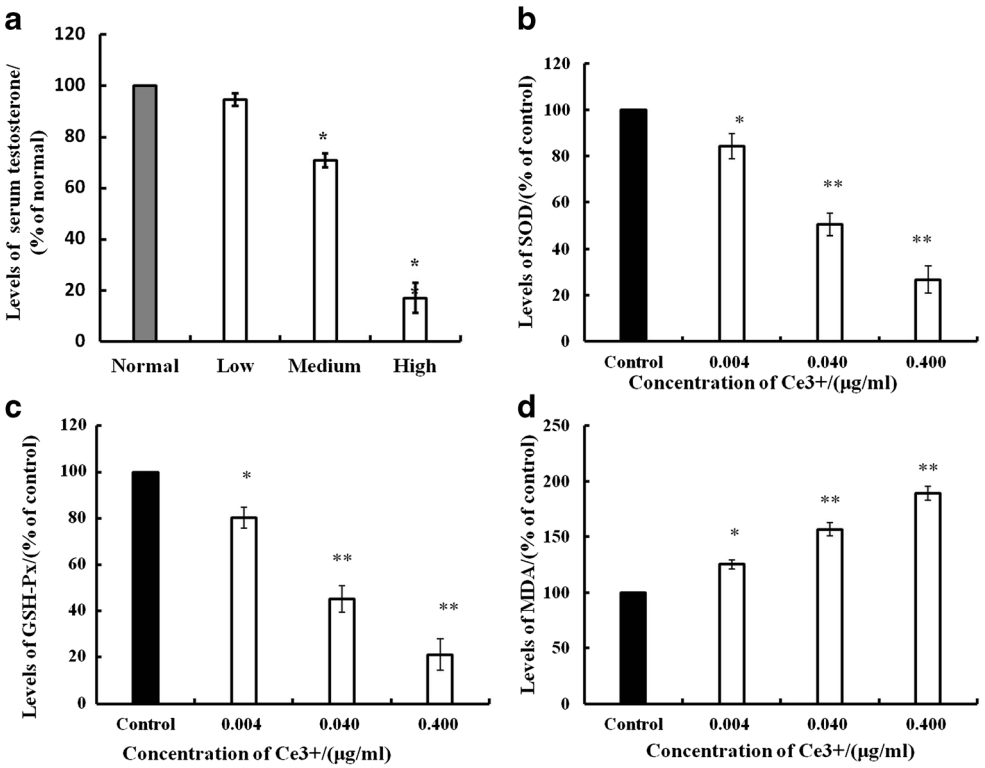

Fig. 3 Effect of rare earths on serum testosterone in male mice and Ce^{3+}-induced oxidative stress on human sperm. The graphic of **a** is the levels of serum testosterone in male mice, and oxidative stress was assessed by measuring SOD (**b**), GSH-Px (**c**), and MDA (**d**). Values are expressed as mean±SD (n=8), $^{*}p<0.05$ and $^{**}p<0.01$ compared to the control group

death. It also implied that excessive rare earth exposure may be a risk factor for infertility or aberration, and its accumulation in the reproductive system intake through the food chain should be under intense scrutiny.

Cell cycle and cell apoptosis of sperm determination

As shown in Fig. 4a, with the large intake of rare earths, the percentage of testis cell number increased in the G_0/G_1 phase, while it decreased in the S and G_2+M phase; the difference of high-dose group was significant ($p<0.05$, compared to the normal group). The same results were tested in the cell apoptosis assay as shown in Fig. 4b.

Raman spectra

Effect on testis in male mice

A typical Raman spectrum of normal testis tissue was shown in Fig. 5. The primary Raman peaks of the normal testis tissue (Fig. 5 normal) were observed at 1,002 cm^{-1} (phenylalanine), 1,042 cm^{-1} (in-plane modes of -C_6H_4-), 1,126 cm^{-1} (−C-N), 1,205 cm^{-1} (deformation vibration of -CH- or -CO-), 1,337 cm^{-1} (stretching of C-C), 1,445 cm^{-1} (stretching of -CH_2- and -CH_3), and 1,658 cm^{-1} (amide I of protein).

All the Raman spectra of the testis tissues have been baseline corrected, smoothed, normalized, and the final spectrum was averaged (Fig. 6). Compared with the normal group,

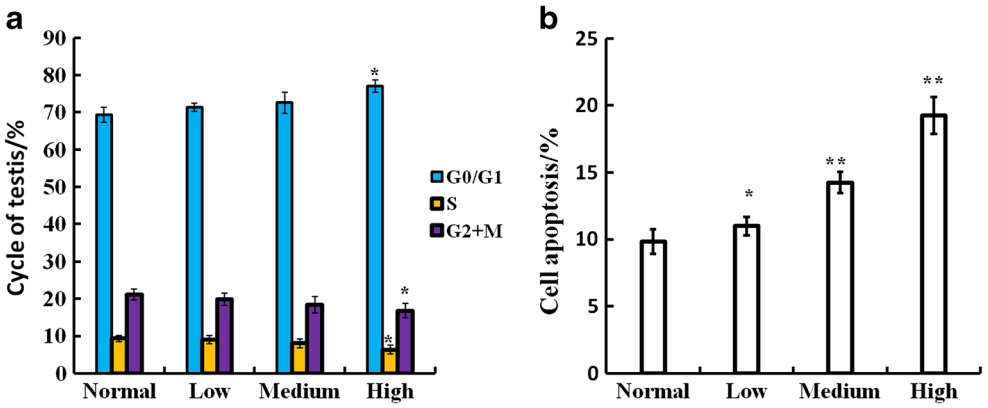

Fig. 4 Effect of rare earths on the cycle and apoptosis of testis in male mice. The graphic of **a** is cycle and **b** is cell apoptosis. Values are expressed as mean± SD (n=8), $^{*}p<0.05$ and $^{**}p<0.001$ compared to the normal group

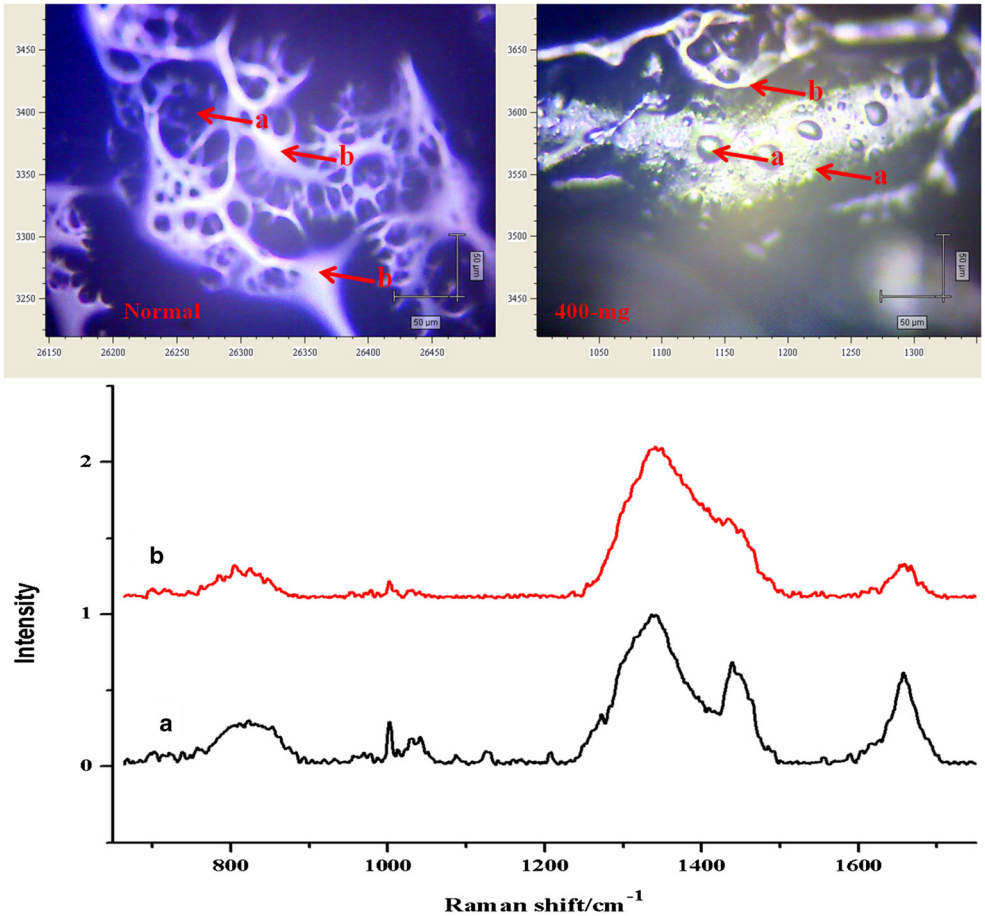

Fig. 5 A typical bright-field optical image with a scale bar of 50 μm and Raman spectra of the seminiferous tubule (**a**) and tunica albuginea (**b**) of the male mice testis

the Raman intensities of rare earth-treated groups changed significantly with peaks of 1,002, 1,126, 1,445, and 1,658 cm^{-1}; much of the peak intensities increased when feed was 100 mg/[kg·day] for 21 days, while the intensities decreased when the dose added up to 200 and 400 mg/[kg·day] except at peaks of 830 and 1,205 cm^{-1} for tunica albuginea, as shown in Fig. 6, which indicated that adequate traces of rare earths were beneficial for the body, while it is of absolutely adverse consequences if excessive.

Effect on human sperm

As shown in Fig. 8, the optical image of a human sperm was attached to a coverslip. The sperm cell has a typical streamlined shape and size, and can be clearly distinguished. So in combination with the corresponding Raman spectra, each of the three main clusters can, unambiguously, be assigned to certain cellular compartments of the sperm cell, as the spectra of sperm DNA shows in Fig. 7.

The sperm spectra showed three broad regions of overlayed peaks at 600–1,100, 1,150–1,550, and 1,550–1,700 cm^{-1} as shown in Fig. 7. Particularly prominent were 10 peaks (677, 787, 856, 993, 1,094, 1,340, 1,376, 1,487, 1,577, and 1,662 cm^{-1}) consistent with the presence of DNA. The sharp peak at 787 $cm^{-1}$was indicative of the backbone phosphodiester group, and 1,094 cm^{-1} was indicative of the PO_4 backbone; peaks at 830–856 cm^{-1} showed that the conformation of the DNA was type B. Peaks at 677, 726, 750, 1,254, 1,305, 1,340, 1,376, 1,421, 1,487, and 1,662 cm^{-1} belonged to the characteristic Raman bases spectra. Peaks at 950, 993, and 1,443 cm^{-1} contributed to the desoxyribose and phosphodiester groups, together with the stretching vibration banding at 1,052 and 1,612 cm^{-1}. The complete Raman frequency assignment of the recorded spectra is presented in Table 1 (Thomas and Kyogoku 1977; Goodwin and Brahms 1978; Xu et al. 1998, 1999; Zhao et al. 1998; Kolodziejski 2013; Wang et al. 2013; Schulze et al. 2013).

As a consequence of the induction of Ce^{3+} nDNA fragmentation, we found major differences in the corresponding Raman spectral profiles, specifically alterations within the full spectral range, which includes the band associated with the DNA phosphate backbone; the changes of the spectra intensities of the exposed groups as compared to those of the normal group; and the changes of the main peak frequency that were presented in Fig. 8 and Table 1.

As shown in Fig. 8, the most relevant peaks in this spectrum were the strong Raman peak at 789 cm^{-1} which has contributions from tyrosine and cytosine vibrations as well as

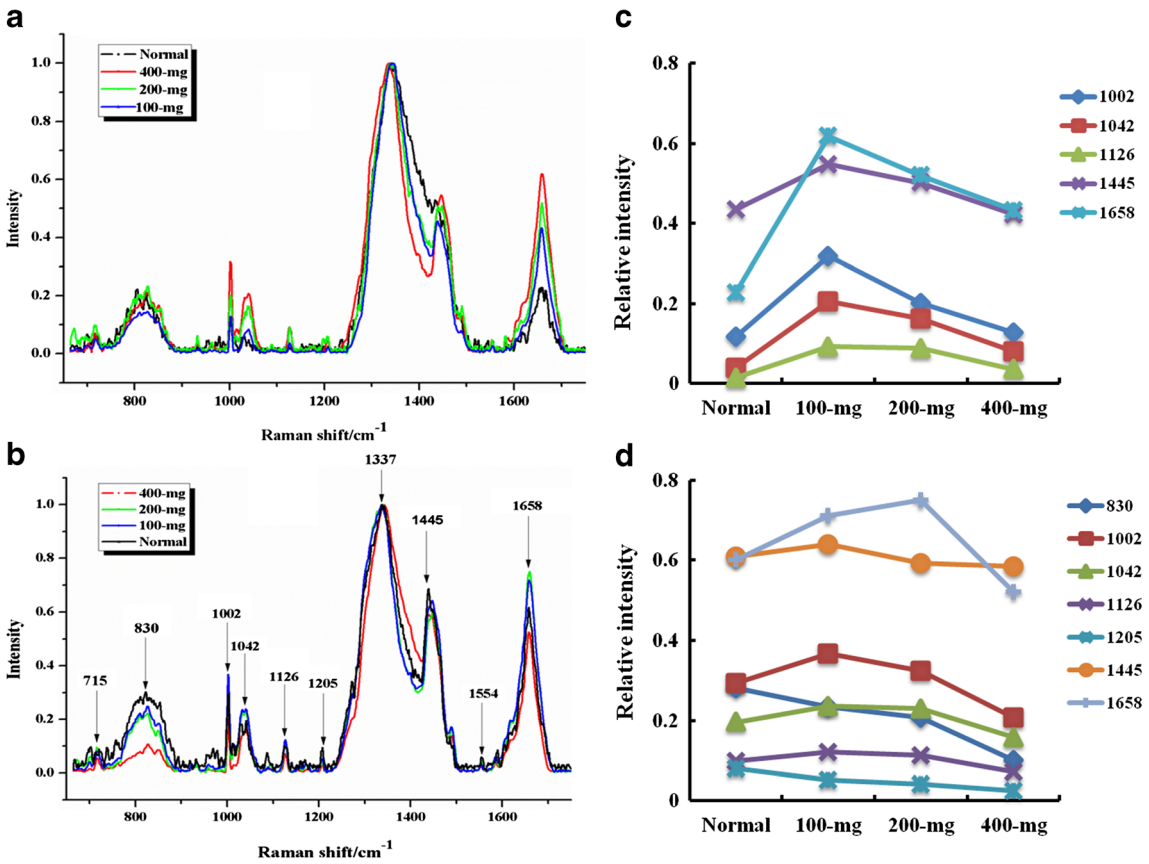

Fig. 6 Raman spectrum of **a** the seminiferous tubule and **b** tunica albuginea of testis which were normalized and averaged from eight samples and five spectra of each sample, and the average spectral intensities of **c** seminiferous tubule and **d** tunica albuginea at some typical Raman peaks

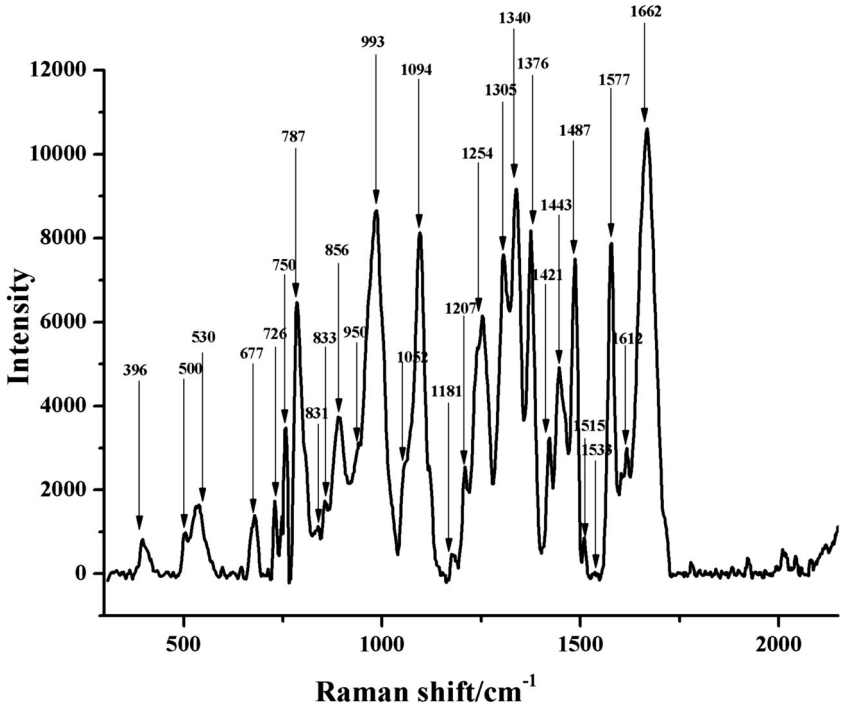

Fig. 7 Raman spectrum of the normal control sperm DNA which was smoothed, normalized, and averaged from eight samples and five spectra of each sample

Table 1 Raman frequencies and assignments of DNA of human sperm

Frequency/cm^{-1}	Assignments	Changes of the frequency/cm^{-1}		
		0.004 $CeCl_3$	0.040 $CeCl_3$	0.400 $CeCl_3$
396	δ (CH, CO)	0	–	–
500	δ (CH, CO)	+2	+3	–
530	δ (CH, CO)	0	−2	−5
677	T	−2	−3	−6
726	A	+2	+5	+6
750	T	−3	+3	+4
787	*str* (OP_2 of diester)	+2	+3	+3
831	B conformation	+2	+2	0
833	B conformation	0	+6	+6
856	B confirmation	0	+3	+5
950	Desoxyribose	+2	+3	+4
993	Desoxyribose	−4	−6	−8
1,052	*v* (C-O of desoxyribose)	−2	−4	−4
1,094	*str* (O=P=o)	−2	−5	−6
1,181	C, G, A,*v* (C-N)	−3	−4	−4
1,207	δ (CH, CO)	+2	+10	+8
1,254	C, A	+3	+5	+4
1,305	A	0	−2	−3
1,340	A	+2	+3	+3
1,376	T, A, G	+4	+5	+5
1,421	A, G	−3	−5	−5
1,443	Desoxyribose	−3	+2	0
1,487	G, A	+2	+3	+2
1,515	A	+1	−1	+1
1,533	G, C	−5	−1	+3
1,577	G, A	0	−2	−1
1,612	δ (CC, CN, CO)	−2	−5	−5
1,662	T, C-O	−3	−6	−10

str symmetrical stretching vibration, *v* stretching vibration, δ deformation vibration, *A* adenine, *G* guanine, *C* cytosine, *T* thymine

from the DNA backbone, the PO_2 backbone vibration at 1,094 cm^{-1}, and the deoxyadenine (dA) vibration at 1,305 cm^{-1}. The sperm cell spectrum (Fig. 8) is characterized by a much weaker peak at 789 cm^{-1} and a strong methylene deformation mode at 1,448 cm^{-1}, as well as additional contributions to the 1,221 cm^{-1} peak due to protein CH_2 twisting vibrations and the 1,612 cm^{-1} peak due to the amide II of protein as shown in Fig. 9.

The rare earths, which has strong biological activities, are uneasy to degrade, and has a long half-life and other physical or chemical properties, were widely used in agriculture, forestry, animal husbandry, fishery, and pharmaceutical chemical industry that is affecting the human health through food chain more and more. Even worse, it has not been proven whether rare earths is the biological essential elements involved in the process and effect of biochemistry, the unclear effect on human health, and the long-term biological effects, which all need urgent solution.

In all of the human body systems, the reproductive system is one of the more sensitive organs for poisonous and harmful material systems, especially as the testes is an organ that can be easily damaged. Sometimes, great harm can be done with only trace amounts of toxic or harmful substances. Previous studies (Levack et al. 2002; Friel et al. 1999) were mainly focused on female reproductive system and embryos, less on the male reproductive system. As reports showed, Ce reduce the rate of pregnant and sperm deformation and the level of serum testosterone. There are several acceptable mechanisms such as (1) testicular cells and vascular system disorder, (2) blood testosterone barrier damage, (3) macromolecules' function deficiency, (4) and hypothalamus-pituitary gland-gonad irregularity. In this study, results showed that for over 200 mg/[kg·day] of the last 3 weeks of the male mice, the weight, testis/body coefficient, levels of LDH, testosterone (Cox and John-Alde 2005; Reed et al. 2006; Mooradian et al. 1987; Morimoto et al. 2013; Yan et al. 2013), SDH (Sikirzhytskaya

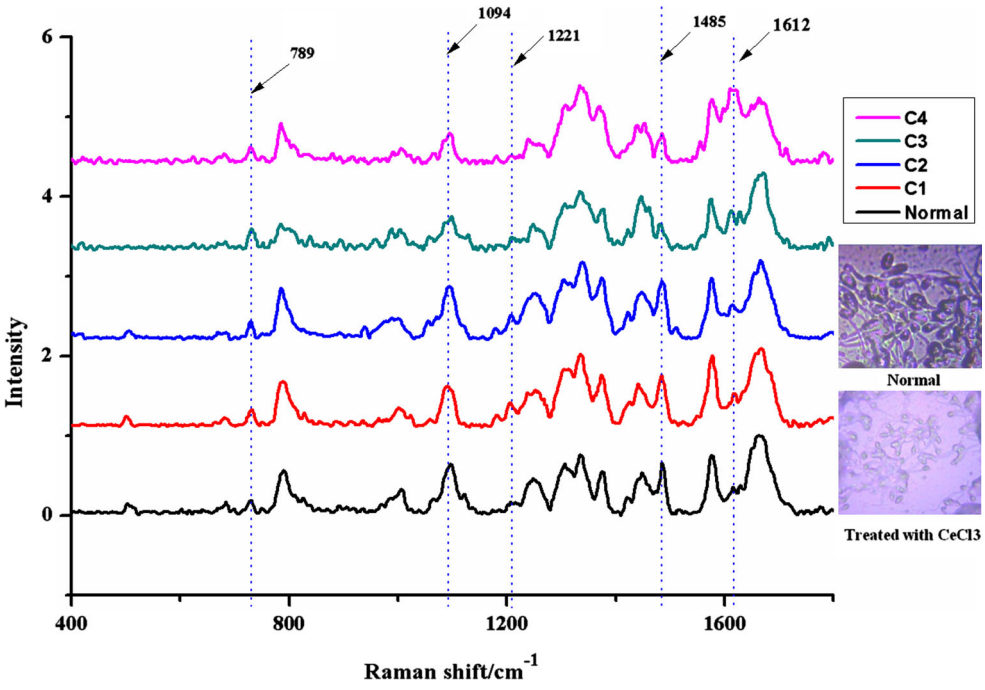

Fig. 8 Images of the human sperm under the 50 times electronic microscope and Raman spectrum of different treated sperm which was smoothed, normalized and averaged from eight samples and five spectra of each sample. *Normal* normal group, *treated* exposed to cerium trichloride ($CeCl_3$) group, *C1* the 0.0004 μg/mL of the Ce^{3+}-treated group, *C2* the 0.0040 μg/mL of the Ce^{3+}-treated group, *C3* the 0.0400 μg/mL of the Ce^{3+}-treated group, and *C4* the 0.4000 μg/mL of the Ce^{3+}-treated group

et al. 2013), SODH, G-6PD, cell cycle changed, and cell apoptosis more or less changed. The level of oxidative stress and chemical component of the human sperm indicated that long-term exposure or ingestion of rare earths will be harmful for the reproductive system; the injury mechanism will influence the oxidative stress and blood testosterone barrier, and, at the same time, combined with the big biomolecule will result in the disabling of its activity and then testicular cells and vascular system disorder. The results also suggested that Ce^{3+} can cause oxidative damage and destroy the antioxidant defense systems of the sperm and even lead to damage or death. It also implied that excessive rare earth exposure may be a risk factor for infertility or aberration, and its accumulation in the reproductive system intake through the food chain should be under intense scrutiny.

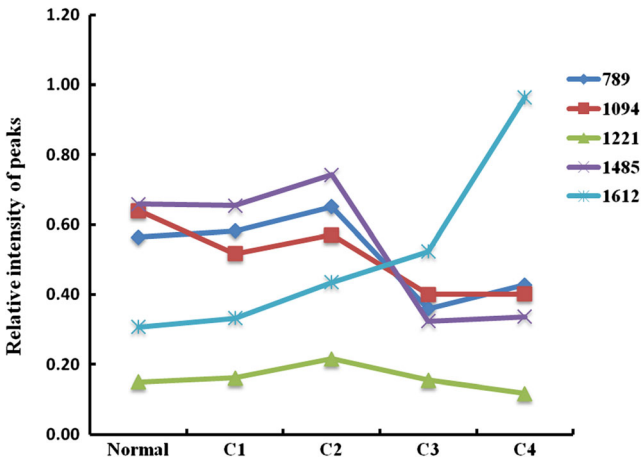

Fig. 9 The relatively intensities of the different treated groups at the main Raman bands, which can be the biological markers that indicates the different levels of damage of Ce^{3+} on human sperm

Confocal micro-Raman spectroscopy, which depends on polarizability change of an oscillating molecule, has proven extremely versatile and led to a vast array of applications across the disciplines of chemistry, physics, biology, biomedicine, engineering, archeology, and been widely used in the field of biomedical science (Kotchey et al. 2013; Adil and Guha 2013; Richard-Lacroix and Pellerin 2013; Zhuang et al. 2012; Caponi et al. 2013; Pudlas et al. 2010; Ellis et al. 2013; Jayawardhana et al. 2013; Won-in et al. 2011; Smith et al. 2013). The micro-Raman spectroscopy has become an ideal method to detect the damage on organs. Previous studies found that micro-Raman spectroscopy can distinguish DNA packaging of normal and abnormal human spermatozoa (Huser et al. 2009; Meister et al. 2010) and combination with the Raman images of human sperm cells in which different subcellular organelles can clearly be identified (Sánchez et al. 2012). The human sperm cell is usually divided into a head, a connecting piece (the neck), a middle piece, and the flagellum. Results of the "Raman fingerprints" of the human sperm DNA exposed to 0.040 mg/ml $CeCl_3$ was very different from that of the normal, the Raman bands at 789 cm^{-1} (backbone phosphodiester), 1,094 cm^{-1} (PO_4 backbone), 1,221 cm^{-1} (methylene deformation mode), 1,485 cm^{-1} (methylene deformation mode), and 1,612 cm^{-1} (amide II), of which intensities and shifts were changed and might be the diagnostic biomarkers or potential therapeutic targets. More studies are needed in this area.

Conclusion

From the changes of weight; testis/body coefficient; levels of LDH, SDH, SODH, G-6PD, and testosterone; cell cycle and cell apoptosis in male mice induced by rare earth; and the level of oxidative stress and chemical component of human sperm caused by Ce^{3+}, we might be sure that long-term or excessive exposure to the rare earths will be harmful for the reproductive system. The injury mechanism might be that the rare earths influence the oxidative stress and blood testosterone barrier and angle the big biomolecule concurrently, which might cause testicular cells and vascular system disorder and/or dysfunction, and, at the same time, might change the physical and chemical properties of the sperm directly.

Acknowledgments The authors thank Hui-qing Zhong, the lab manager of MOE Key Laboratory of Laser Life Science & Institute of Laser Life Science, College of Biophotonics, South China Normal University.

Conflict of interests The authors declare that they have no conflict of interests.

References

Adil D, Guha S (2013) Surface-enhanced Raman spectroscopic studies of the Au-pentacene interface: a combined experimental and theoretical investigation. J Chem Phys 139:044715

Aly HA, Azhar AS (2013) Methoxychlor induced biochemical alterations and disruption of spermatogenesis in adult rats. Reprod Toxicol 40: 8–15

Boenigk J, Wiedlroither A, Pfandl K (2005) Heavy metal toxicity and bioavailability of dissolved nutrients to a bacterivorous flagellate are linked to suspended particle physical properties. Aquat Toxicol 71: 249–259

Caponi S, Liguori L, Giugliarelli A, Mattarelli M, Morresi A, Sassi P, Urbanelli L, Musio C (2013) Raman micro-spectroscopy: a powerful tool for the monitoring of dynamic supramolecular changes in living cells. Biophys Chem 182:58–63

Cox RM, John-Alder HB (2005) Testosterone has opposite effects on male growth in lizards (*Sceloporus* spp.) with opposite patterns of sexual size dimorphism. J Exp Biol 208:4679–4687

Ellis DI, Cowcher DP, Ashton L, O'Hagan S, Goodacre R (2013) Illuminating disease and enlightening biomedicine: Raman spectroscopy as a diagnostic tool. Analyst 138:3871–3884

Fan G, Yuan Z, Zheng H, Liu Z (2004) Study on the effects of exposure to rare earth elements and health-responses in children aged 7–10 years. Wei Sheng Yan Jiu 33:23–28

Friel JK, Andrews WL, Jackson SE, Longerich HP, Mercer C, McDonald A, Dawson B, Sutradhar B (1999) Elemental composition of human milk from mothers to premature and full-term infants during the first 3 months of lactation. Biol Trace Elem Res 67:225–247

Gardner AM, Xu FH, Fady C, Jacoby FJ, Duffey DC, Tu Y, Lichtenstein A (1997) Apoptotic versus nonapoptotic cytotoxicity induced by hydrogen peroxide. Free Radic Biol Med 22:73–83

Goodwin DC, Brahms J (1978) Form of DNA and the nature of interactions with protein in chromatin. Nucleic Acids Res 5:835–850

He Y, Xue L (2005) Biological effects of rare earth elements and their action mechanisms. Ying Yong Sheng Tai Xue Bao 16:1983–1989

He J, Mi N, Kuang YC, Fan QY, Wang X, Guan W, Li GH, Li CS, Wang XW (2004) Speciation and distribution characters of rare earth elements in the Baotou Section of the Yellow River. Huan Jing Ke Xue 25:61–66

Huser T, Wilson B, Matthews DL (2009) Biophotonics and regenerative medicine—ideal partners for research in the 21(st) century. J Biophotonics 2:613–614

Jayawardhana S, Rosa L, Juodkazis S, Stoddart PR (2013) Additional enhancement of electric field in surface-enhanced Raman scattering due to Fresnel mechanism. Sci Rep 3:2335

Jiang DG, Yang J, Zhang S, da Yang J (2012) A survey of 16 rare earth elements in the major foods in China. Biomed Environ Sci 25:267–271

Kolodziejski N (2013) Tip-enhanced Raman spectroscopy for the base interrogation of DNA. Methods Cell Biol 114:611–628

Kotchey GP, Gaugler JA, Kapralov AA, Kagan VE, Star A (2013) Effect of antioxidants on enzyme-catalysed biodegradation of carbon nanotubes. J Mater Chem B Mater Biol Med 1:302–309

Levack VM, Hone PA, Phipps AW, Harrison JD (2002) The placental transfer of cerium: experimental studies and estimates of doses to the human fetus from 141Ce to 144Ce. Int J Radiat Biol 78:227–235

Liu D, Wang X, Chen Z (2012) Effects of rare earth elements and REE-binding proteins on physiological responses in plants. Protein Pept Lett 19:198–202

Liu JJ, Han D, Liu Y (2013a) Study on the contents and fractionation of rare earth elements in filtering water and suspensions in Gansu, Ningxia and Inner Mongolia Sections of Yellow River by HR-ICP-MS. Guang Pu Xue Yu Guang Pu Fen Xi 33:1116–1121

Liu JJ, Lai ZJ, Liu Y (2013b) Study on speciation and fractionation of rare earth elements in surface sediments in Gansu, Ningxia and Inner Mongolia sections of Yellow River. Guang Pu Xue Yu Guang Pu Fen Xi 33:798–803

Liu PH, Rui YK, Ye CS (2007) Effects of soil on the concentration of rare earth in Nanfeng orange. Guang Pu Xue Yu Guang Pu Fen Xi 27: 2575–2577

Li Y, Yang JL, Jiang Y (2012) Trace rare earth element detection in food and agricultural products based on flow injection walnut shell packed microcolumn preconcentration coupled with inductively coupled plasma mass spectrometry. J Agric Food Chem 60:3033–3041

Meister K, Schmidt DA, Bründermann E, Havenith M (2010) Confocal Raman microspectroscopy as an analytical tool to assess the mitochondrial status in human spermatozoa. Analyst 135:1370–1374

Mooradian AD, Morley JE, Korenman SG (1987) Biological actions of androgens. Endocr Rev 8:1–28

Morimoto H, Iwata K, Ogonuki N, Inoue K, Atsuo O, Kanatsu-Shinohara M, Morimoto T, Yabe-Nishimura C, Shinohara T (2013) ROS are required for mouse spermatogonial stem cell self-renewal. Cell Stem Cell 12:774–786

Pang X, Li D, Peng A (2002) Application of rare-earth elements in the agriculture of China and its environmental behavior in soil. Environ Sci Pollut Res Int 9:143–148

Pant N, Prasad AK, Srivastava SC, Shankar R, Srivastava SP (1995) Effect of oral administration of carbofuran on male reproductive system of rat. Hum Exp Toxicol 14:889–894

Peng RL, Pan XC, Xie Q (2003) Relationship of the hair content of rare earth elements in young children aged 0 to 3 years to that in their mothers living in a rare earth mining area of Jiangxi. Zhonghua Yu Fang Yi Xue Za Zhi 37:20–22

Pudlas M, Koch S, Bolwien C, Walles H (2010) Raman spectroscopy as a tool for quality and sterility analysis for tissue engineering applications like cartilage transplants. Int J Artif Organs 33:228–237

Reed WL, Clark ME, Parker PG, Raouf SA, Arguedas N, Monk DS, Snajdr E, Nolan V, Ketterson ED (2006) Physiological effects on demography: a long-term experimental study of testosterone's effects on fitness. Am Nat 167:667–683

Richard-Lacroix M, Pellerin C (2013) Novel method for quantifying molecular orientation by polarized Raman spectroscopy: a comparative simulations study. Appl Spectrosc 67:409–419

Sánchez V, Redmann K, Wistuba J, Wübbeling F, Burger M, Oldenhof H, Wolkers WF, Kliesch S, Schlatt S, Mallidis C (2012) Oxidative DNA damage in human sperm can be detected by Raman microspectroscopy. Fertil Steril 98:1124–9.e1-3

Schulze HG, Konorov SO, Piret JM, Blades MW, Turner RF (2013) Label-free imaging of mammalian cell nucleoli by Raman microspectroscopy. Analyst 138:3416–3423

Sikirzhytskaya A, Sikirzhytski V, McLaughlin G, Lednev IK (2013) Forensic identification of blood in the presence of contaminations using Raman microspectroscopy coupled with advanced statistics: effect of sand, dust, and soil. J Forensic Sci 58:1141–1148

Smith ZJ, Huser TR, Wachsmann-Hogiu S (2013) Raman scattering in pathology. Stud Health Technol Inform 185:207–234

Su DZ, Xiang LD, Zhai YX (1993) Studies on the rare earth content in food and its daily intake in man. Zhonghua Yu Fang Yi Xue Za Zhi 27:6–9

Thomas GJ Jr, Kyogoku Y (1977) Biological Science: infrared and Raman spectroscopy part. Jr. Bram CEG, Grasselli JG (eds). Dekker, USA, 717–872

Tong SL, Zhu WZ, Gao ZH, Meng YX, Peng RL, Lu GC (2004) Distribution characteristics of rare earth elements in children's scalp hair from a rare earth mining area in southern China. J Environ Sci Health A Tox Hazard Subst Environ Eng 39:2517–2532

Traina ME, Rescia M, Urbani E, Mantovani A, Macrì C, Ricciardi C, Stazi AV, Fazzi P, Cordelli E, Eleuteri P, Leter G, Spanò M (2003) Long-lasting effects of lindane on mouse spermatogenesis induced by in utero exposure. Reprod Toxicol 17:25–35

Wang L, He D, Zeng J, Guan Z, Dang Q, Wang X, Wang J, Huang L, Cao P, Zhang G, Hsieh J, Fan J (2013) Raman spectroscopy, a potential tool in diagnosis and prognosis of castration-resistant prostate cancer. J Biomed Opt 18:87001

Wei Z, Yin M, Zhang X, Hong F, Li B, Tao Y, Zhao G, Yan C (2001) Rare earth elements in naturally grown fern *Dicranopteris linearis* in relation to their variation in soils in south Jiangxi region (southern China). Environ Pollut 114:345–355

Wei ZL, Rui YK, Tian ZH (2009) Content of rare earth elements in wild *Hypericum japonicum* Thunb. Guang Pu Xue Yu Guang Pu Fen Xi 29:1696–1697

Won-in K, Thongkam Y, Pongkrapan S, Intarasiri S, Thongleurm C, Kamwanna T, Leelawathanasuk T, Dararutana P (2011) Raman spectroscopic study on archaeological glasses in Thailand: ancient Thai glass. Spectrochim Acta A Mol Biomol Spectrosc 83:231–235

Wu M, Huang S, Wen W, Sun X, Tang X, Scholz M (2011) Nutrient distribution within and release from the contaminated sediment of Haihe River. J Environ Sci (China) 23:1086–1094

Xu YM, Zhang ZY, Zhang HY (1998) Raman spectroscopic study of DNA after photosensitive damage caused by hypocrellin A and B. Sci China C Life Sci 41:360–366

Xu YM, Zhou ZX, Yang HY, Xu Y, Zhang ZY (1999) Raman spectroscopic study of microcosmic photodamage of the space structure of DNA sensitized by Yangzhou hematoporphyrin derivative and photofrin II. J Photochem Photobio B: Biology 52:30–34

Xu Y, Song J, Duan L, Li X, Yuan H, Li N, Zhang P, Zhang Y, Xu S, Zhang M, Wu X, Yin X (2012) Fraction characteristics of rare earth elements in the surface sediment of Bohai Bay, North China. Environ Monit Assess 184:7275–7292

Yan F, Shrestha YK, Spurgeon CL (2013) Determination of ferric ions using surface-enhanced Raman scattering based on desferrioxamine-functionalized silver nanoparticles. Chem Commun (Camb) 49:7962–7964

Yu L, Dai YC, Yuan ZK, Li J (2004) Effects of rare earth compounds on human peripheral mononuclear cell telomerase and apoptosis. Zhonghua Yu Fang Yi Xue Za Zhi 38:248–251

Yu L, Dai Y, Yuan Z, Li J (2007) Effects of rare earth elements on telomerase activity and apoptosis of human peripheral blood mononuclear cells. Biol Trace Elem Res 116:53–59

Zhang FS, Yamasaki S, Kimura K (2001) Rare earth element content in various waste ashes and the potential risk to Japanese soils. Environ Int 27:393–398

Zhang H, Deng L, Yang J, Jiang J, Shen Z, Xie J (2009) Rare earth elements in marine organisms from Shenzhen coastal region. Wei Sheng Yan Jiu 38:543–545

Zhang S, Shan XQ (2001) Speciation of rare earth elements in soil and accumulation by wheat with rare earth fertilizer application. Environ Pollut 112:395–405

Zhao HX, Xu YM, Zhang ZY (1998) Raman spectroscopic study of DNA photodamage sensitized by hypocrellin B and 5-brominated-hypocrellin B. Chin Sci Bull 43:1128–1234

Zhou J, Guo L, Xiao W, Geng Y, Wang X, Shi X, Dan S (2012) Physiological effects of rare earth elements and their application in traditional Chinese medicine. Zhongguo Zhong Yao Za Zhi 37: 2238–2241

Zhou X, Wang B, Chen Y, Mao Z, Gao C (2013) Uptake of cerium oxide nanoparticles and their influences on functions of A549 cells. J Nanosci Nanotechnol 13:204–215

Zhuang ZF, Li N, Gou ZY, Zhu MF, Xiong K, Chen SJ (2012) Study of molecule variations in renal tumor based on confocal micro-Raman spectroscopy. J Bio Optics 18:031103